LETTER Communicated by Helge Ritter

Breaking Rotational Symmetry in a Self-Organizing Map Model for Orientation Map Development

M. Riesenhuber
Department of Brain and Cognitive Sciences and Center for Biological and Computational Learning, Massachusetts Institute of Technology, E25-221, Cambridge, MA 02139, U.S.A.

H.-U. Bauer
D. Brockmann
T. Geisel
Max-Planck-Institut für Strömungsforschung, Postfach 28 53, 37018 Göttingen, Federal Republic of Germany

We analyze the pattern formation behavior of a high-dimensional self-organizing map (SOM) model for the competitive projection of ON-center-type and OFF-center-type inputs to a common map layer. We mathematically show, and numerically confirm, that even isotropic stimuli can drive the development of oriented receptive fields and an orientation map in this model. This result provides an important missing link in the spectrum of pattern formation behaviors observed in SOM models. Extending the model by including further layers for binocular inputs, we also investigate the combined development of orientation and ocular dominance maps. A parameter region for combined patterns exists; corresponding maps show a preference for perpendicular intersection angles between iso-orientation lines and ocularity domain boundaries, consistent with experimental observations.

1 Introduction

Topographic maps are a ubiquitous pattern of organization in the brain. Among the most intensely investigated such patterns are orientation maps and ocular dominance maps in the visual cortex. Various models have been formulated that generate topographic maps as a consequence of activity-driven self-organization processes (for two recent reviews, see Erwin, Obermayer, & Schulten, 1995; Swindale, 1996). The simulated maps coincide with observed maps in many aspects. Yet distinctive differences remain between simulated and observed maps, as well as between simulated maps from different modeling frameworks. The better we can relate such differences to specific underlying assumptions, the more differences we can eliminate, and the more experimental observations we can account for within uni-

versal modeling frameworks, the more stable our understanding of map self-organization processes will become.

A few years ago, two map formation models were presented that generate oriented receptive fields from a competition of ON-center and OFF-center cell responses in the lateral geniculate nucleus (LGN) (Miller, 1992, 1994; Miyashita & Tanaka, 1992). These models elegantly explain how orientation-selective simple cell responses could be due to a self-organization process driven by nonpatterned input activity and could take place even before birth. Without discussing any of the details of these models, we note that their inputs are nonoriented, yet the resulting patterns break this symmetry.

A third, rather widely applied framework for map development is Kohonen's self-organizing map (SOM) algorithm. SOM-based models have sucessfully accounted for various aspects of visual (Obermayer, Ritter, & Schulten, 1990; Obermayer, Blasdel, & Schulten, 1992; Goodhill, 1993; Wolf, Bauer, & Geisel, 1994; Wolf, Bauer, Pawelzik, & Geisel, 1996; Bauer, Brockmann, & Geisel, 1997), auditory (Martinetz, Ritter, & Schulten, 1988) and somatosensory (Ritter & Schulten, 1986; Andres, Schlüter, Spengler, & Dinse, 1994) map formation. Yet in simulations of SOM-based models for ON-center- and OFF-center-cell competition, a break of rotational symmetry has not been observed so far, despite a lengthy search by several groups. This negative outcome could be the consequence of a suboptimal selection of parameters, or it could be the fingerprint of a fundamental difference between SOM-based models and the models by Miyashita and Tanaka, and by Miller. Clarification of this issue is an interesting problem, not only with regard to explanations of orientation map development but, in particular, with regard to theoretical consistency between modeling frameworks.

In this article, we report that SOMs can break rotational symmetry, albeit in a quite small regime of parameters. Using a recently described analysis technique (Riesenhuber, Bauer, & Geisel, 1996; Bauer et al., 1997), we first mathematically analyze the pattern formation behavior of the corresponding SOM model. After a brief introduction to the SOM in the second section, we describe analytical results in the third section. Guided by the mathematical analysis, we also performed simulations of the model; the results are given in the fourth section. Finally, we investigate the development of combined orientation and ocular dominance maps.

2 "High-Dimensional" SOM Model for the Development of Orientation Maps from Nonoriented Stimuli

Neurons in an SOM are characterized by positions $\mathbf{r}$ in a map lattice $\mathcal{A}$ and receptive fields $\mathbf{w_r}$ in a map input space $\mathcal{V}$. The input space is assumed to consist of one (or several) layer(s) of input channels. The typically large number of input channels give rise to the notion of a high-dimensional SOM, as opposed to a feature map description. As a consequence, stimuli $\mathbf{v} \in \mathcal{V}$ are activity distributions, and receptive fields $\mathbf{w_r}$ are synaptic weight distri-

butions. A stimulus $\mathbf{v}$ is mapped onto that neuron $\mathbf{s} \in \mathcal{A}$, whose receptive field $\mathbf{w_s}$ matches $\mathbf{v}$ best,

$$\mathbf{s} = \arg\max_{\mathbf{r}\in\mathcal{A}}\{\mathbf{w_r} \cdot \mathbf{v}\}. \tag{2.1}$$

Presenting a random sequence of stimuli and performing adaptation steps,

$$\Delta\mathbf{w_r} = \epsilon h(\mathbf{r} - \mathbf{s})(\mathbf{v} - \mathbf{w_r}), \tag{2.2}$$

the internal shape of individual receptive fields as well as the map layout self-organize simultaneously. The neighborhood function $h(\mathbf{r} - \mathbf{s})$,

$$h(\mathbf{r} - \mathbf{s}) = \exp\left(-\frac{\|\mathbf{r} - \mathbf{s}\|^2}{2\sigma^2}\right), \tag{2.3}$$

ensures that neighboring neurons align their receptive fields; that is, it imposes topography on the map. A comprehensive treatment of many theoretical and application-related aspects of SOMs can be found in Ritter, Martinetz, and Schulten (1992) and Kohonen (1995).

Within this general framework, we now consider a projection geometry analogous to that proposed by Miller (1992, 1994) and Miyashita and Tanaka (1992). Cells in ON-center and OFF-center input layers project to the map layer. As would result from a filtering of pointlike retinal stimuli by thalamic ON-center and OFF-center cells, we assume our stimuli to consist of an activity peak in one layer, plus an activity annulus in the other layer.

Mathematically, stimuli are represented as difference-of-gaussians (DOG) (stimulus center position: $\mathbf{x_0}$, widths of the two gaussians: $\sigma_{1,2}$, relative amplitude of the gaussians: k),

$$\mathbf{a}(\mathbf{x}; \mathbf{x}_0) = \exp\left(\frac{-\|\mathbf{x} - \mathbf{x}_0\|^2}{2\sigma_1^2}\right) - k\exp\left(\frac{-\|\mathbf{x} - \mathbf{x}_0\|^2}{2\sigma_2^2}\right). \tag{2.4}$$

Furthermore, $\mathbf{a}_\bullet(\mathbf{x}; \mathbf{x}_0) = [\mathbf{a}(\mathbf{x}; \mathbf{x}_0)]_+$ denotes the activity distribution of the central peak of the DOG, and $\mathbf{a}_\circ(\mathbf{x}; \mathbf{x}_0) = [-\mathbf{a}(\mathbf{x}; \mathbf{x}_0)]_+$ the annulus-shaped activity distribution corresponding to the negative part of the DOG ($[\cdot]_+$ is the rectification operator). Naturally, ON-type and OFF-type stimuli are represented as two-component vectors,

$$\mathbf{v}_{\mathrm{ON}} = (\mathbf{a}_\bullet, \mathbf{a}_\circ), \quad \mathbf{v}_{\mathrm{OFF}} = (\mathbf{a}_\circ, \mathbf{a}_\bullet), \tag{2.5}$$

each component describing the (nonnegative) activity distribution in one of the input layers. In the simulations, the center positions $\mathbf{x_0}$ and polarity (that is, whether the stimulus is $\mathbf{v}_{\mathrm{ON}}$ or $\mathbf{v}_{\mathrm{OFF}}$) are chosen at random.

3 Mathematical Results on the Formation of Oriented Receptive Fields

Recently, Riesenhuber et al. (1996) and Bauer et al. (1997) described a new technique to calculate conditions on stimulus and map parameters for the emergence of nontrivial patterns in high-dimensional SOMs. This technique makes use of a distortion measure $E_{\mathbf{v}}$, which is evaluated for different potentially stable states of the map and is assumed to be minimized by the SOM algorithm. A crucial feature of the method is the way in which "potentially stable states" of a SOM are formalized. Although an explicit characterization of such states in terms of the weight vectors $\mathbf{w_r}$ seems impossible without actually simulating the SOM, the states can also be characterized by the way they distribute stimuli among map neurons (the tesselation). This is specific to the SOM, where the winner-take-all mapping rule (see equation 2.1) assigns a particular map neuron to each stimulus.

Denoting by $\Omega_{\mathbf{r}}$ all stimuli that are mapped to neuron $\mathbf{r}$ (the Voronoi cell of $\mathbf{r}$), we define a distortion measure,

$$E_{\mathbf{v}} = \sum_{\mathbf{r},\mathbf{r}'} h(\mathbf{r} - \mathbf{r}')\, w(\mathbf{r}, \mathbf{r}'), \tag{3.1}$$

$$w(\mathbf{r}, \mathbf{r}') = \sum_{\mathbf{v}\in\Omega_{\mathbf{r}}} \sum_{\mathbf{v}'\in\Omega_{\mathbf{r}'}} (\mathbf{v} - \mathbf{v}')^2. \tag{3.2}$$

Each term in $E_{\mathbf{v}}$ consists of the mean squared difference $w(\mathbf{r}, \mathbf{r}')$ between stimuli within the same, or between neighboring, Voronoi cells, weighted by the neighborhood function $h(\mathbf{r} - \mathbf{r}')$. The definition of $E_{\mathbf{v}}$ is motivated by the analogy of SOMs to vector quantizers (see Riesenhuber et al., 1996). Qualitatively different states of a map yield different values of $E_{\mathbf{v}}$ because they correspond to different tesselations $\{\Omega_{\mathbf{r}}\}$. What are the typical tesselations in the present context?

To simplify the analysis, we assume an equal number of ON-center input channels, OFF-center input channels, and map neurons, with a basically retinotopic projection. We further assume that the stimulus center positions $\mathbf{x}_0$ are constrained to the positions of the input channels, resulting in twice as many stimuli as map neurons. Three qualitatively different possible map states can be distinguished:

1. System $\mathcal{B}$: Each neuron responds to both an ON- and an OFF-stimulus, each located at the same retinal position. This tesselation yields neurons with orientation-insensitive receptive fields.
2. System $\mathcal{S}$: As in system $\mathcal{B}$, each neuron responds to stimuli of both polarities, but now displaced one step along one retinal coordinate. The displacement breaks isotropy. It causes the receptive fields to exhibit internal ON-center and OFF-center structure, with orientation specificity.

3. System $\mathcal{O}$: Each neuron responds to two retinally neighboring stimuli of identical polarity. Although this tesselation induces an orientation specificity, it also breaks the symmetry between ON-center and OFF-center inputs to each neuron. Neurons segregate into ON-center- and OFF-center-dominated populations, analogous to an ocular dominance map. While this state is an imaginable (and numerically observed, see below) state of SOMs, we do not consider this state as biologically interesting.

To evaluate $w(\mathbf{r}, \mathbf{r}')$ and $E_{\mathbf{v}}$ for these tesselations, we need to consider the difference δ^s between two stimuli of same polarity, separated by a distance of $\Delta\mathbf{x}_0 = \mathbf{x}_0 - \mathbf{x}'_0$,

$$\delta^s(\Delta\mathbf{x}_0) = \sum_{\mathbf{x}} \left(\mathbf{a}_\bullet(\mathbf{x}, \mathbf{x}_0) - \mathbf{a}_\bullet(\mathbf{x}, \mathbf{x}'_0)\right)^2 + \left(\mathbf{a}_\circ(\mathbf{x}, \mathbf{x}_0) - \mathbf{a}_\circ(\mathbf{x}, \mathbf{x}'_0)\right)^2, \quad (3.3)$$

and the difference δ^a between two oppositely polarized stimuli,

$$\delta^a(\Delta\mathbf{x}_0) = \sum_{\mathbf{x}} \left(\mathbf{a}_\bullet(\mathbf{x}, \mathbf{x}_0) - \mathbf{a}_\circ(\mathbf{x}, \mathbf{x}'_0)\right)^2 + \left(\mathbf{a}_\circ(\mathbf{x}, \mathbf{x}_0) - \mathbf{a}_\bullet(\mathbf{x}, \mathbf{x}'_0)\right)^2. \quad (3.4)$$

Using these distances, and exploiting the isotropy with respect to one retinal coordinate, we obtain for the interaction terms w (see equation 3.2):

$$w^{\mathcal{B}}(\Delta r) = \delta^s(\Delta r) + \delta^a(\Delta r), \quad (3.5)$$

$$w^{\mathcal{S}}(\Delta r) = \delta^s(\Delta r) + \frac{1}{2}\{\delta^a(\Delta r - 1) + \delta^a(\Delta r + 1)\}, \quad (3.6)$$

$$w^{\mathcal{O}}(\Delta r) = \sum_{i=s,a} \frac{1}{2}\delta^i(\Delta r) + \frac{1}{4}\{\delta^i(\Delta r + 1) + \delta^i(\Delta r - 1)\}. \quad (3.7)$$

Inserting equations 3.5–3.7 into equation 3.1 and performing a numerical summation, we obtain the distortion measures $E^{\mathcal{B}}_{\mathbf{v}}$, $E^{\mathcal{S}}_{\mathbf{v}}$, and $E^{\mathcal{O}}_{\mathbf{v}}$. This analysis predicts that, depending on the stimulus parameters $\sigma_{1,2}$, k, and the map neighborhood parameter σ, different final states of the map will be attained. Figure 1a shows a state diagram in the σ, k-plane, at widths $\sigma_1 = 1$, $\sigma_2 = 2$. At large values of the annulus amplitude k, receptive fields segregate into "monopolar" ON- and OFF-receptive fields. Large values of the neighborhood width σ prohibit internal structure of the receptive fields to occur. Only in a rather small regime of σ, k-values, the biologically interesting map state $\mathcal{S}$ is attained.

4 Numerical Results

To corroborate the mathematical analysis above and to obtain orientation maps, we also investigated the model numerically. In a first series we ran

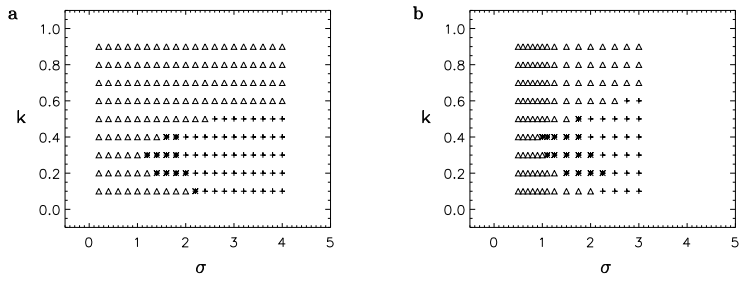

Figure 1: Analytical (a) and numerical (b) phase diagrams for the SOM orientation map model. The parameters σ and k denote the neighborhood width of the SOM algorithm and the annulus amplitude of the stimuli, respectively. $+$: the nonoriented state $\mathcal{B}$. $\star$: the oriented state $\mathcal{S}$. $\triangle$: the (nonbiological) state $\mathcal{O}$. In both diagrams, further parameters were $\sigma_1 = 1$, $\sigma_2 = 2$, in the numerical maps we applied 10^5 learning steps, learning step size was decreased from $\epsilon_{\text{init}} = 0.2$ to $\epsilon_{\text{final}} = 0.01$, and the neighborhood width σ was kept constant during the simulation.

simulations with 16×16 neuron maps, at various values of σ and k. Classifying the resulting receptive fields with regard to the states $\mathcal{B}, \mathcal{S}, \mathcal{O}$, we obtained the state diagram depicted in Figure 1b, which corresponds quite well to the mathematically obtained diagram.

To obtain receptive fields with a fine spatial resolution, we also simulated maps with 48×48-channel input layers, projecting to a 24×24-neuron map layer. Figure 2 shows exemplary receptive fields of neurons in a 4×8 segment of the map. The receptive fields show a multilobed structure and are clearly oriented. The variation of orientation over the whole map is shown in an angle map in Figure 3, where the preferred orientation of each cell is given by a circular color code. As in orientation maps obtained by optical imaging methods in the cat (Bonhoeffer & Grinvald, 1991) or monkey (Blasdel & Salama, 1986), we find a patchy arrangement of different preferred orientations and also pinwheel-like singularities.

In addition to the map of preferred orientation angles of the receptive fields, we also calculated the phases of the receptive field, that is, the shift angles that would occur in a Gabor function fit to the receptive field profile (see the caption for Figure 3). It has been hypothesized that the phase angle is also arranged in a topographic fashion in the primary visual cortex, with a topology of the combined orientation and phase stimulus space equivalent to that of a Klein bottle (Tanaka, 1995). In our simulated maps, we find the phase angle to vary indeed in a smooth way in many areas of the map (see the arrows in Figure 3). Phase and orientation values are not correlated.

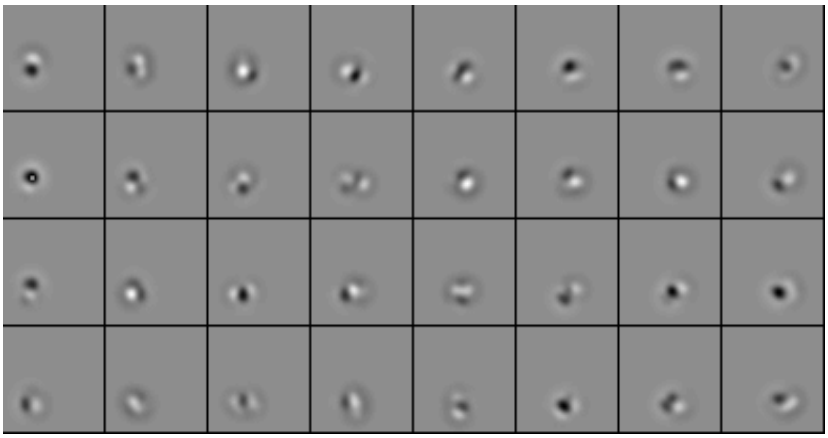

Figure 2: Sample receptive fields of an SOM orientation map (4×8 segment of a 24×24-neuron SOM, with two 48×48 input layers, periodic boundary conditions). Further parameters of the simulation were: $\sigma_1 = 3.4$, $\sigma_2 = 6.8$, $k = 0.3$, width of SOM neighborhood function $\sigma = 0.85$, 3×10^5 learning steps, $\epsilon = 0.1 \rightarrow 0.01$. For each neuron, the difference between ON-center and OFF-center cell layer connection strengths is shown as a gray-value image. The gray background means no connection strength; black and white regions indicate preferred connections to the ON- or OFF-center layers.

2π-singularities can be found in the phase, at locations other than those of orientation singularities. All the topological properties we could identify in our map are consistent with Tanaka's suggestion of the Klein bottle topology.

5 Development of Combined Orientation and Ocular Dominance Maps

Finally, we complemented the two ON-center and OFF-center input cell layers for one eye by two further ON-center and OFF-center cell layers for the other eye. The repertoire of possible patterns in this extended model should go beyond merely oriented receptive fields in an orientation map. It should also include monocular receptive fields and ocular dominance maps, and combinations of the two types of patterns.

Stimuli in the extended model consist of activity distributions in all four input layers. Although the difference in the shape of the activity distributions between ON-center and OFF-center layers is the same as before, the partial stimuli are assumed to be of identical shape in the corresponding

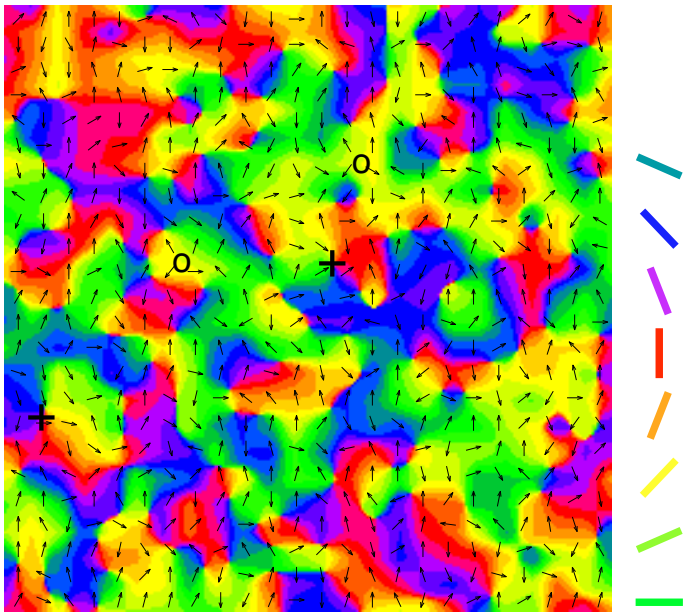

Figure 3: The complete map described in the caption of Figure 2, now depicted as an angle map using a circular color code for the preferred orientation angles of each cell. Superimposed on the color-coded orientation map, we show (as arrows) the phase angle of the receptive fields. The phase angle is calculated by rotating each receptive field by the inverse of its preferred orientation (so that the lobes of an ideal bilobed receptive would fall on different sides of the horizontal meridian after rotation) and then determining the phase shift as compared to a dampened sine wave (i.e., a Gabor filter) of the receptive field profile. A rightward arrow designates a phase of zero degrees, that is, the receptive field is bilobed with the positive lobe being in the upper hemisphere after rotation. An upward arrow represents a phase angle of 90 degrees, that is, a trilobed receptive field with the negative lobe in the middle. Crosses and circles show examplary locations of orientation and phase singularities, respectively.

layers for either eye, but attenuated by a factor of c, $0 \leq c \leq 1$, in one of the eyes (analogous to the assumptions underlying a recently analyzed SOM-based model for ocular dominance formation; Bauer et al., 1997; see also Goodhill, 1993). This yields, apart from the random variations of the

stimulus center, four different types of stimuli:

$$\mathbf{v}_{\mathrm{L,ON}} = \begin{pmatrix} \mathbf{a}_\bullet \\ \mathbf{a}_\circ \\ c \cdot \mathbf{a}_\bullet \\ c \cdot \mathbf{a}_\circ \end{pmatrix}, \quad \mathbf{v}_{\mathrm{L,OFF}} = \begin{pmatrix} \mathbf{a}_\circ \\ \mathbf{a}_\bullet \\ c \cdot \mathbf{a}_\circ \\ c \cdot \mathbf{a}_\bullet \end{pmatrix},$$
$$\mathbf{v}_{\mathrm{R,ON}} = \begin{pmatrix} c \cdot \mathbf{a}_\bullet \\ c \cdot \mathbf{a}_\circ \\ \mathbf{a}_\bullet \\ \mathbf{a}_\circ \end{pmatrix}, \quad \mathbf{v}_{\mathrm{R,OFF}} = \begin{pmatrix} c \cdot \mathbf{a}_\circ \\ c \cdot \mathbf{a}_\bullet \\ \mathbf{a}_\circ \\ \mathbf{a}_\bullet \end{pmatrix}. \tag{5.1}$$

The analysis technique introduced in section 3 can be applied to this more complicated case as well, considering the different tesselation possibilities for four stimuli per neuron. To save space, we omit the details of the rather lengthy calculations and proceed to a description of the results. Since we have five parameters in the model now (σ_1, σ_2, k for the DOG, c for the between-eye correlations, and σ as a map control parameter), the full state diagram cannot be depicted. Instead, we show in Figure 4a a section in the k-c-plane. Regions with orientation only and with ocular dominance only are found. Most important, there is a region with a combination of both orientation and ocular dominance at small values of k and c.

In computer simulations, we found maps with monocular receptive fields, oriented receptive fields, or combined monocular, oriented receptive fields, each in the parameter regimes predicted by the analysis (see Figure 4b). Figure 5 shows one combined map in a plot that displays the boundaries of the iso-ocularity domains superimposed on the color-coded orientation map.

Determining the transition lines between iso-ocularity regions in the simulated map, and computing the intersection angles with the iso-orientation lines at these locations, we compiled an angle histogram (see Figure 6). Iso-orientation lines intersect the boundaries between iso-ocularity regions preferably at larger angles, consistent with experimental observations by Bartfeld and Grinvald (1992) and Obermayer and Blasdel (1993).

6 Discussion

We showed mathematically and numerically how in a high-dimensional SOM model for the competitive projection of ON-center and OFF-center inputs to a common map layer, a rotation symmetry of stimuli can be broken to yield oriented receptive fields. This pattern formation behavior can be described only in a high-dimensional map formation framework, which also allows consideration of the internal structure of receptive fields. In low-

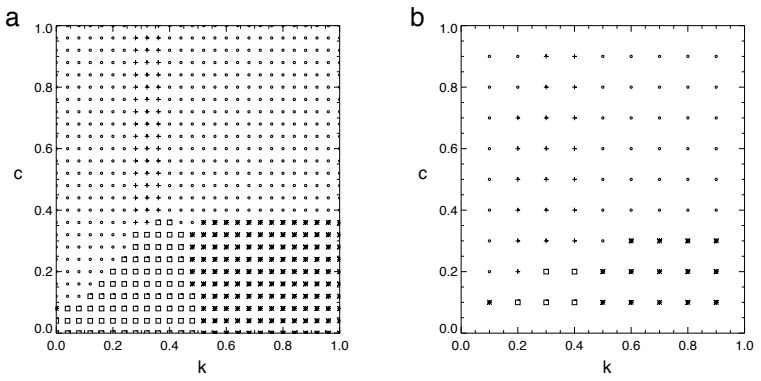

Figure 4: Phase diagram for combined orientation and ocular dominance maps, as a function of ON-OFF stimulus parameter k and between-eye-correlation parameter c, at $\sigma_1 = 0.84$, $\sigma_2 = 1.68$, $\sigma = 1.0$. $\circ$: states with unoriented receptive fields. $+$: oriented, binocular receptive fields. $\star$: monocular receptive fields with type $\mathcal{O}$ ON-center OFF-center cell segregation. $\square$: monocular, oriented receptive fields. (a) The analytically obtained diagram. (b) The diagram resulting from classification of the receptive fields of simulated maps.

dimensional feature map models, where each map dimension corresponds to a particular stimulus and receptive field parameter, a nontrivial structure along a particular dimension cannot be obtained if the stimuli have no extension along this dimension (as is the case for round stimuli with respect to an orientation dimension). A break of isotropy has already been observed in other frameworks for map development models (Miyashita & Tanaka, 1992; Miller, 1992, 1994). The results we describe here for the SOM framework close a somewhat puzzling gap in the qualitative behavior of these different frameworks, reducing the relative importance of the specific mathematical formalizations, and increasing the importance of common mechanisms.

Our results are based not only on numerical simulations but also on a mathematical analysis. The coincidence of the mathematically derived parameter regimes for particular map structures and the numerical observation of these structures underlines the value of our energy formalism to analyze pattern formation in high-dimensional SOM models and to guide simulations of these models. For the case of combined ocular dominance and orientation maps, the analysis turned out to involve a substantially larger number of map patterns, which need to be considered. The increase in effort necessary for the two-variable case suggests that this kind of analysis is not feasible for maps with three underlying symmetries. For the com-

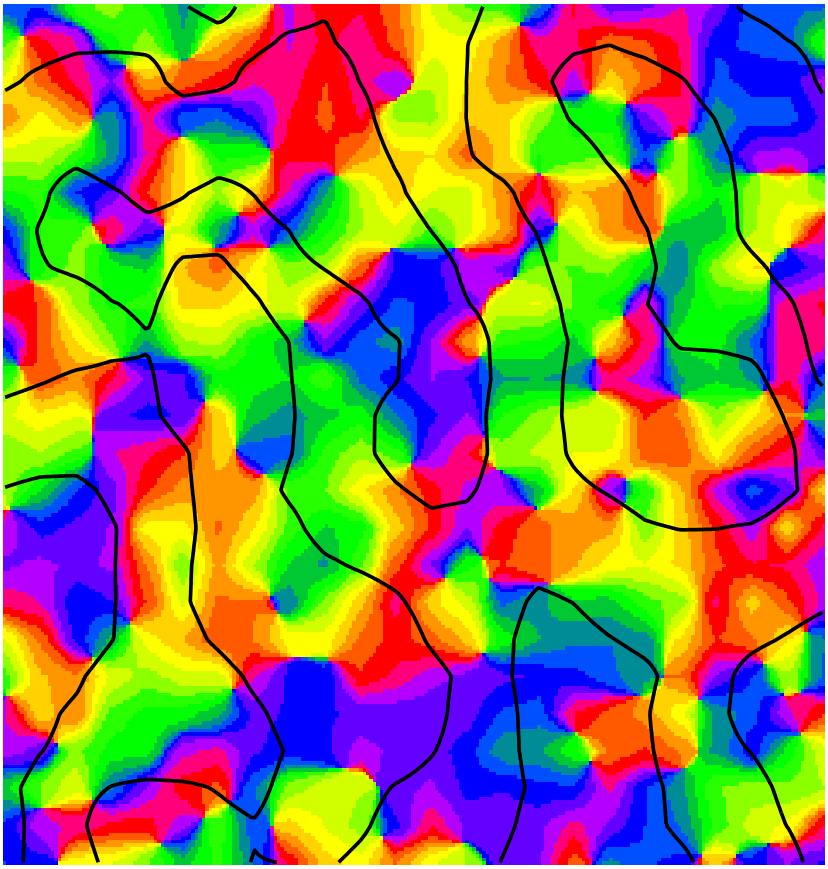

Figure 5: Combined ocular dominance and orientation map, with stimulus parameters as described in the caption of Figure 4. The orientation angle map is given in color code (as in Figure 3); the iso-ocularity domain boundaries are superimposed as black lines. Further parameters are: 24×24-neuron SOM, 34×34-channel input layers, $\sigma = 0.71$, 3×10^5 learning steps, $\epsilon = 0.1 \rightarrow 0.01$, periodic boundary conditions.

bined maps, we identified a parameter regime in which ocular dominance and orientation structure stably coexist. In the correlation-based framework, combined maps were numerically found to exist (Erwin & Miller, 1995), but the mathematical underpinnings were judged controversial (Piepenbrock, Ritter, & Obermayer, 1996, 1997).

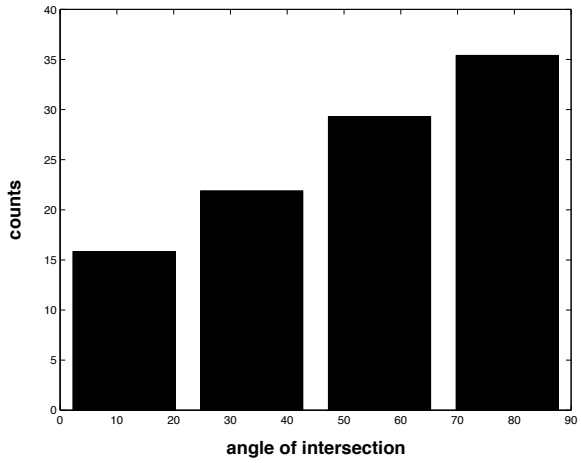

Figure 6: Histogram of angle of intersection of iso-orientation lines and iso-ocularity domain boundaries, computed for all cells along iso-ocularity domain boundaries of the map shown in Figure 5.

Acknowledgments

We gratefully acknowledge interesting discussions with Ken Miller and Fred Wolf. This work has been supported by the Deutsche Forschungsgemeinschaft through Sonderforschungsbereich 185 Nichtlineare Dynamik, TP E6.

References

Andres, M., Schlüter, O., Spengler, F., & Dinse, H. R. (1994). A model of fast and reversible representational plasticity using Kohonen mapping. In M. Marinao & P. G. Morasso (Eds.), *Proceedings of the ICANN94, Sorrento* (pp. 306–309). Berlin: Springer-Verlag.

Bartfeld, E., & Grinvald A. (1992). Relationship between orientation preference pinwheels, cytochrome oxidase blobs and ocular-dominance columns in primate striate cortex. *Proc. Nat. Acad. Sci. USA*, *89*, 11905–11909.

Bauer, H.-U., Brockmann, D., & Geisel, T. (1997). Analysis of ocular dominance pattern formation in a high-dimensional self-organizing-map-model. *Network*, *8*, 17–33.

Blasdel, G. G., & Salama, G. (1986). Voltage-sensitive dyes reveal a modular organization in monkey striate cortex. *Nature*, *321*, 579–585.

Bonhoeffer, T., & Grinvald, A. (1991). Iso-orientation domains in cat visual cortex are arranged in pinwheel-like patterns. *Nature*, *353*, 429–430.

Erwin, E., & Miller, K. D. (1995). Modeling joint development of ocular dominance and orientation maps in primary visual cortex. In J. Bower (Ed.), *Computational neuroscience* (pp. 179–184). Boston: Kluwer.

Erwin, E., Obermayer, K., & Schulten, K. (1995). Models of orientation and ocular dominance columns in the visual cortex: A critical comparison. *Neur. Comp.*, *7*, 425–468.

Goodhill, G. J. (1993). Topography and ocular dominance: A model exploring positive correlations. *Biol. Cyb.*, *69* 109–118.

Kohonen, T., (1995). *The self-organizing map*. Berlin: Springer-Verlag.

Martinetz, T., Ritter, H., & Schulten, K. (1988). Kohonen's self-organizing map for modeling the formation of the auditory cortex of a bat. In SGAICO-Proceedings "Connectionism in Perspective," 403–412.

Miller, K. D. (1992). Development of orientation columns via competition between ON- and OFF-center inputs. *NeuroRep.*, *3*, 73–79.

Miller, K. D. (1994). A model for the development of simple-cell receptive fields and the ordered arrangement of orientation columns through activity dependent competition between On- and Off-center inputs. *J. Neurosci.*, *14*, 409–441.

Miyashita, M., & Tanaka, S. (1992). A mathematical model for the self-organization of orientation columns in visual cortex. *NeuroRep.*, *3*, 69–72.

Obermayer, K., & Blasdel, G. G. (1993). Geometry of orientation and ocular dominance columns in monkey striate cortex. *J. Neurosci.*, *13*, 4114–4129.

Obermayer, K., Blasdel, G. G., & Schulten, K. (1992). Statistical-mechanical analysis of self-organization and pattern formation during the development of visual maps. *Phys. Rev. A*, *45*, 7568–7569.

Obermayer K., Ritter, H., & Schulten, K. (1990). A principle for the formation of the spatial structure of cortical feature maps. *Proc. Nat. Acad. Sci. USA*, *87*, 8345–8349.

Piepenbrock, C., Ritter, H., & Obermayer, K. (1996). Linear correlation-based learning models require a two-stage process for the development of orientation and ocular dominance. *Neur. Proc. Lett.*, *3*, 1–7.

Piepenbrock, C., Ritter, H., & Obermayer, K. (1997). The joint development of orientation and ocular dominance: Role of constraints. *Neur. Comp.*, *9*, 959–970.

Riesenhuber, M., Bauer, H.-U., & Geisel, T. (1996). Analyzing phase transitions in high-dimensional self-organizing maps. *Biol. Cyb.*, *75*, 397–407.

Ritter, H., Martinetz, T., & Schulten, K., (1992). *Neural computation and self-organizing maps*. Reading, MA: Addison-Wesley.

Ritter, H., & Schulten, K. (1986). On the stationary state of Kohonen's self-organizing sensory mapping. *Biol. Cyb.*, *54*, 99–106.

Swindale, N. V. (1996). The development of topography in the visual cortex: A review of models. *Network*, *7*, 161–247.

Tanaka, S. (1995). Topological analysis of point singularities in stimulus preference maps of the primate visual cortex. *Proc. R. Soc. London B*, *261*, 81–88.

Wolf, F., Bauer, H.-U., & Geisel, T. (1994). Formation of field discontinuities and islands in visual cortical maps. *Biol. Cyb.*, *70*, 525–531.
Wolf, F., Bauer, H.-U., Pawelzik, K., & Geisel, T. (1996). Organization of the visual cortex. *Nature*, *382*, 306–307.

Received May 6, 1997; accepted September 18, 1997.